IUST Iran University of Science and Technology

Iranian Journal of Electrical and Electronic Engineering

Journal Homepage: ijeee.iust.ac.ir

Research Paper

A Novel Non-Entropic Objective Function for Multilevel Optimal Threshold Selection Using Adaptive Equilibrium Optimizer

G. Das*, R. Panda*(C.A.), L. Samantaray**, and S. Agrawal*

Abstract: Multilevel optimal threshold selection is important and comprehensively used in the area of image processing. Mostly, entropic information-based threshold selection techniques are used. These methods make use of the entropy of the distribution of the grey levels of an image. However, entropy functions largely depend on spatial distribution of the image. This makes the methods inefficient when the distribution of the grey information of an image is not uniform. To solve this problem, a novel non-entropic method for multilevel optimal threshold selection is proposed. In this contribution, simple numbers (pixel counts), explicitly free from the spatial distribution, are used. A novel non-entropic objective function is proposed. It is used for multilevel threshold selection by maximizing the partition score using the adaptive equilibrium method. A new theoretical derivation for the fitness function is highlighted. The key to the achievement is the exploitation of the score among classes, reinforcing an improvised threshold selection process. Standard test images are considered for the experiment. The performances are compared with state-of-the-art entropic value-based methods used for multilevel threshold assortment and are found better. It is revealed that the results obtained using the suggested technique are encouraging both qualitatively and quantitatively. The newly proposed method would be very useful for solving different real-world engineering optimization problems.

Keywords: Artificial Intelligence, Entropic Methods, Equilibrium Optimizer, Multilevel Threshold Selection.

1 Introduction

ANALYSIS of an image needs proper partition into meaningful regions. In this connection, multilevel threshold selection plays a key role in digital image processing [1]. Multilevel thresholding methods are used for partitioning an image into many classes. Multiple threshold values are needed for the purpose. This kind of method is more suitable to partition images with complex boundaries and multimodal histograms. This is the reason why multilevel thresholding is an important area of research. To be precise, the significance of the method is primarily to partition the image into several distinct regions, which correspond to one background and many objects. Thresholding method is one of the easiest and most efficient techniques used in image segmentation. It groups the pixels of an image into various classes built on their intensity levels. The key issue in the threshold selection process is to compute optimal threshold values. The various threshold selection algorithms established so far are classified into six categories, which depend on 1) shape of the image histogram, 2) clustering measurement of the feature space, 3) entropic value-based information from the histogram, 4) information

Iranian Journal of Electrical and Electronic Engineering, 2022.
Paper first received 04 July 2021, revised 18 December 2021, and accepted 15 January 2022.
* The authors are with the Department of Electronics and Telecommunication Engineering, VSS University of Technology, Burla - 768018, Odisha, India.
E-mails: gyanesh_das@rediffmail.com, rpanda_etc@vssut.ac.in, and agrawals_72@yahoo.com.
** The author is with the Department of Electronics and Communication Engineering, Ajaya Binaya Institute of Technology, Cuttack, Odisha, India.
E-mail: leena_sam@redeffmail.com.
Corresponding Author: R. Panda.
https://doi.org/10.22068/IJEEE.18.2.2230

regarding image attributes, 5) image spatial information; 6) image's local characteristics [2]. The entropic value-based threshold selection for image segmentation is considered to be an efficient method. The class of entropy-based thresholding algorithms makes use of the entropy of the distribution of the grey levels in an image which is derived from Shannon's entropy from information theory. Many entropic value-based threshold selection algorithms have been proposed [3-12]. For example, minimum cross entropy thresholding method [5], maximum cross entropy method [6], Masi entropy [8-10], Renyi entropy [11], Kapur's entropy [13] Otsu's method [13], and Tsallis entropy-based method [14] to name a few. Pun [15] utilized the maximum entropic value as an optimum criterion for threshold selection. Sezgin and Sankur [2] offered a survey over various threshold selection methodologies and their quantitative performance evaluation. Lei and Fan [14] described a comparative analysis of entropic and relative entropic-value-based threshold selection schemes. Eight different entropic-value-based information-theoretic techniques are described thoroughly. Shape and uniformity features are used for an evaluation of these methods. In this review, the authors concluded that the information carried by the image histogram is not adequate for the selection of a proper threshold value, because these methods do not consider spatial correlation information at all. Therefore, images having similar histograms may show the same threshold values. Further, more or less, the performances of the entropy-based techniques very much depend on the spatial distribution of the grey levels. Especially, when the spatial domain distribution of the grey information of an image is not uniform. Thus, it makes the methods inefficient due to their dependency on spatial domain distribution.

This has motivated us to research an efficient methodology for selection of optimum threshold values to capture changes between grey levels. Furthermore, we are motivated to efficiently capture image shred boundaries, which is essential for improvising the threshold selection enactment. A new objective function is proposed in this paper. The idea is then extended for multilevel threshold selection. Recently, various heuristic computing techniques are proposed for exhaustive search. Equilibrium optimizer (EO) has been proved to be the best among its clan [16]. In this work, we are motivated to use a newly proposed state-of-the-art optimizer called the adaptive equilibrium optimized (AEO) [17], which is an improved version of the EO. The proposed objective function is optimized using the AEO. This contribution may enrich the artificial intelligence (AI) application to multilevel thresholding. For a fair comparison, state-of-the-art methodologies for multilevel thresholding application are also considered in this work. The results, presented in the result section, reveal that the suggested scheme outperforms the state-of-the-art methods. In summary, it is focused on the comparative performance study using two distinct state-of-the-art methods. For instance, non-extensive Tsallis entropy-based technique [14], Otsu method [13]; and the proposed method. It is to be noted that we have implemented Otsu's method for comparison.

The organization of the paper is given as: Section 2 discusses the idea of a score (new objective function) and the proposed methodology. Section 3 describes the concept of the adaptive equilibrium optimization technique. Section 4 presents the results and discussions. Section 5 includes the concluding remarks.

2 Proposed Method

In this section, new theoretical investigations are carried out. A novel objective function is suggested to validate our claim that our technique is better than the entropic value-based methods. The empirical formulation of the problem is explained below. Let $I \in \Re^N$ is an image with N number of pixels, where the intensity values range from 0 to 255. There is a strong need to compute optimal threshold values for accurate segmentation of the image under consideration I. In this context, it is wise to maximize the fitness function (score) among other classes (regions). Firstly, let us consider bi-level thresholded image as $S \in \{0, 1\}^N$ using Otsu's method. It is noteworthy to mention here that the optimal threshold T, achieved from Otsu's method, is used to partition image I into 2 (two) distinct classes, say S_0 and S_1. Class 0 consists of pixels with grey values ranging from 0 to T, while Class 1 consists of pixels with grey levels ranging from T+1 to 255. Let S_k decides whether the k-th pixel belongs to class 0 or 1. Now, SSE stands for the sum of squared errors, and it is a statistical calculation that leads to other data values. When we have a group of data values, it is useful to know how closely these values are related. The difference between the measurement and the mean is called the error. Thus, the sum of squared error (SSE) computed from the partitioned image S is written as:

$$SSE = \sum_{S_k=0} (I_k - \mu_0)^2 + \sum_{S_k=1} (I_k - \mu_1)^2 \quad (1)$$

where I_k denotes the intensity of the k-th pixel in class 0 or 1, $\mu_0 = \sum_{S_k=0} \frac{I_k}{n_S}, \mu_1 = \sum_{S_k=1} \frac{I_k}{(N - n_S)}$ indicate the mean values of class 0 and 1, respectively. Here, n_s denotes the number of pixels in class 0. Note that N represents the total number of pixels. The total number of pixels in class 1 is equal to (N–n_s). It is noteworthy to mention here that the error is to be minimized for achieving the best partitioning of the image. Therefore, the error (E) in the segmentation process is expressed as:

$$E = \| I \|_2^2 - \frac{1}{n_S}\left(\sum_{S_k=0} I_k\right)^2 - \frac{1}{(N - n_S)}\left(\sum_{S_k=1} I_k\right)^2 \quad (2)$$

It is wise to reiterate that ||.||$_2$ represents the standard l_2 norm of the input image. The second term and the third term denote the respective norms of class 0 and class 1, respectively. Note that the 2nd and 3rd terms are computed from the segmented (output) image. When subtracted from the input image, then gives error. Ultimately, Eq. (2) is used to compute the error in segmentation. It is implicit that the normalization of the 2nd and 3rd terms is done using the respective pixel counts. This enhances the knowledge in computing the segmentation error from a bi-level thresholded image.

For further simplification of (2), we assume here the 2nd and the 3rd term to be equal. Thus, Eq. (2) can be simplified as:

$$E = \| I \|_2^2 - \frac{N}{n_S(N-n_S)}\left(\sum_{S_k=0} I_k\right)^2 \tag{3}$$

The assumption in (2) and (3) is taken just to simplify it to develop the theoretical formulation for the partition score. The equation for the partition score is developed assuming the two classes have the same number of pixels initially. However, in real-world images, the number of pixels in the two classes may vary. In theoretical developments, usually assumptions are made to simplify the problem initially. This, in turn, helps us to extend the idea in deriving the practical equations for the multilevel thresholding of digital images.

Therefore, the minimization of the error leads to the maximization of the 2nd term in (3). Following the above justification, we define the newly proposed partition score as:

$$\psi_{I,T} = \max_{S\in\{0,1\}^N} \frac{N}{n_S(N-n_S)}\left(\sum I_k\right) \tag{4}$$

Interestingly, the partition score depends on the threshold value T. To ensure the best outcomes, the partition score value needs to be maximized. Since our motivation is to propose a new methodology for multilevel threshold selection, we have extended the idea to solve the problem.

Multilevel threshold values are used to partition image I into K classes S_1, S_2, …, S_K by selecting threshold values t_1, t_2, …, t_{K-1}. Here, the value of the threshold t_0 is *0* and that of t_K is L–1. For a clear understanding, the block diagram of the suggested methodology is displayed in Fig. 1.

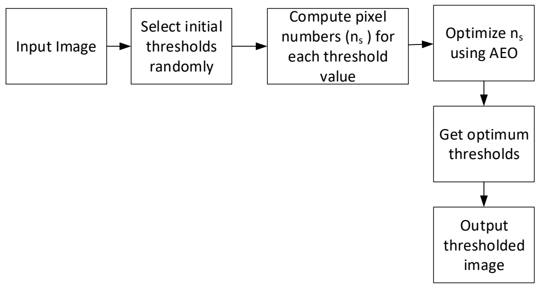

Fig. 1 Block diagram of the suggested method.

The partition score ($\psi_{I,T}$) values are computed using (4). These values are used to obtain optimum threshold values. New objective functions are introduced in this section. The idea is to maximize the multiple functional *f*(.) for achieving optimal thresholds. To be more precise, the main focus is to achieve the best n_s count. Hence, the problem dimension rests on the number of thresholds. This has further inspired us to deploy an adaptive heuristic optimizer that maximizes individual entities in a population of solutions. This has warranted us to suggest novel objective functions that are appropriate for heuristic search methods. The threshold selection approach used here is basically a maximization of the objective function proposed in (5). To figure out, this is the prime contribution. The optimal threshold values are obtained by maximizing the objective function given below:

$$\left[t_{1opt}, t_{2opt}, \ldots, t_{(k-1)opt}\right] = \arg\max_{S\in\{1,\ldots,K\}} \left\{ f\left(n_{S_1}, n_{S_2}, \ldots, n_{S_{(k-1)}}\right)\right\} \tag{5}$$

subject to the following constraints

$$0 < t_{1opt} < t_{2opt} < \cdots < t_{(k-1)opt} < L-1 \tag{6}$$

Need to mention here that the threshold values found are optimal, while the summation over n_s is maximized. The class pixels n_s are maximized using the adaptive equilibrium optimizer. Note that the number of population is fixed here at 30. It is noteworthy to mention here that the search dimension depends on the number of threshold values. The maximum iterations need to be fixed. The objective function value is to be initialized. Subsequently, solutions, i.e. n_s are randomly chosen. Finally, the solution with the best objective function value is considered as the best solution here. Another contribution of this paper is the extension of the above idea of the bi-level threshold selection to multilevel thresholding. Multilevel threshold selection equations are derived and presented in this section. The multiple optimal threshold values are computed by using the following equations:

$$t_{1opt} = \arg\max_{S\in\{1,\ldots,K\}} \left(\left(\frac{N}{n_S(N-n_S)}\right) \sum_{i=0}^{n_{S_1}} \sum_{j=n_{S_1}+1}^{n_{S_2}} \left(I_{i,j}\right) \right) \tag{7}$$

$$t_{2opt} = \arg\max_{S\in\{1,\ldots,K\}} \left(\left(\frac{N}{n_S(N-n_S)}\right) \sum_{i=n_{S_1}+1}^{n_{S_2}} \sum_{j=n_{S_2}+1}^{n_{S_3}} \left(I_{i,j}\right) \right) \tag{8}$$

$$t_{(k-1)opt} = \arg\max_{S\in\{1,\ldots,K\}} \left(\left(\frac{N}{n_S(N-n_S)}\right) \sum_{i=n_{S_{(k-2)}}+1}^{n_{S_{(k-1)}}} \sum_{j=n_{S_{(k-1)}}+1}^{N-n_{S_{(k-1)}}} \left(I_{i,j}\right) \right) \tag{9}$$

Note that n_s in the above equations (7) to (9)

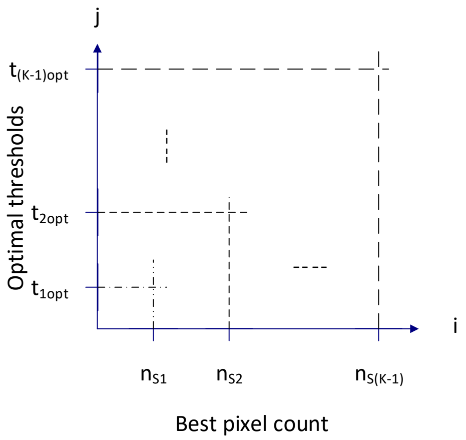

Fig. 2 Idea behind the proposed method.

represents the maximum number of pixels (count) among the different segments (classes). $I_{i,j}$ represents the pixel intensity values in that region.

In the above equations, $n_{S_1}, n_{S_2}, \ldots, n_{S_{(K-1)}}$ denote class pixel counts pertaining to multiple thresholds. Note that the best values for $n_{S_1}, n_{S_2}, \ldots, n_{S_{(K-1)}}$ are obtained deploying the AEO. Then the corresponding thresholds are computed using (7)-(9). It is reiterated that the threshold values achieved are optimal while the partition score is maximized. The multiple threshold computation procedure is shown in Fig. 2.

Nonetheless, $n_{S_1}, n_{S_2}, \ldots, n_{S_{(K-1)}}$ are simple numbers (pixel counts), explicitly free from the spatial dispersal. Furthermore, they help us to partition the image efficiently, because they are computed among different classes in such a manner that the shred boundary between different classes is enshrined. Even more interesting phenomena are that they provide the corresponding optimal thresholds. Intuitively speaking, the problem on hand is primarily a maximization problem. It is good enough to maximize the functional f(.) as discussed above. Nevertheless, it is an exhaustive search issue. Hence, a heuristic search method is suggested. In this connection, the newly proposed ideas are described in this section. The AEO is deployed to maximize the proposed functional f(.). For a comparison, Tsallis non-extensive entropy [14] and Otsu method-based multilevel threshold selection [13] algorithms are also implemented here. The scheme is quite similar to the methodology based on the sum of the maximum entropic values suggested in [7]. However, the non-extensive Tsallis entropy ideas (modified as per the information-theoretic point of view) are used here [14].

Let there be G grey levels in a given image and these gray levels are in the range {1, 2, …, G}. Here, $p_i = p_1, p_2, \ldots, p_g$ are called the probability distributions. From these distributions, specific probability distributions for two different classes, class A and class B, are derived. These distributions for class A and Class B are provided separately by $p_A = \frac{p_1}{P^A}, \frac{p_2}{P^A}, \ldots, \frac{p_t}{P^A}$, $p_B = \frac{p_{t+1}}{P^B}, \frac{p_{t+2}}{P^B}, \ldots, \frac{p_G}{P^B}$, where $P^A = \sum_{i=1}^{t} p_i$, and $P^B = \sum_{i=t+1}^{G} p_i$.

The aim is to maximize the objective function for bi-level thresholding:

$$T_{opt} = \arg\max[S_q^A(t) + S_q^B(t) + (1-q)\cdot S_q^A(t)\cdot S_q^B(t)] \quad (10)$$

where q is the index (entropy value-based) called Tsallis parameter, $S_q^A(t) = \frac{1-\sum_{i=1}^{t}\left(\frac{p_i}{P^A}\right)^q}{q-1}$, $S_q^B(t) = \frac{1-\sum_{i=t+1}^{G}\left(\frac{p_i}{P^B}\right)^q}{q-1}$.

The information measure between the two classes (object and background) is maximized. The corresponding grey value required to maximize them is reflected as the optimum threshold. This method can also be extended to multi-level thresholding as follows: The multilevel optimum threshold selection criterion is organized as an m-dimensional optimization Task. Need to mention here that for computation of 'm' optimal threshold values, [T_1, T_2, …, T_m], the focus is to maximize the fitness function as given below:

$$[T_1, T_2, \ldots, T_m] = \arg\max[S_q^A(t) + S_q^B(t) + \cdots + S_q^m(t) + (1-q)\times S_q^A(t)\times S_q^B(t)\times\cdots\times S_q^m(t)] \quad (11)$$

where $S_q^A(t) = \frac{1-\sum_{i=1}^{t_1}\left(\frac{p_i}{P^A}\right)^q}{q-1}$, $S_q^B(t) = \frac{1-\sum_{i=t_1+1}^{t_2}\left(\frac{p_i}{P^B}\right)^q}{q-1}$, and $S_q^m(t) = \frac{1-\sum_{i=t_m+1}^{G}\left(\frac{p_i}{P^m}\right)^q}{q-1}$.

The aim of AEO is to optimize the objective functions given by (11). The details of the Otsu method are available in [13].

3 The Adaptive Equilibrium Optimizer

Equilibrium Optimizer (EO) is discussed in [16]. This is a state-of-the-art optimization algorithm encouraged by control volume mass balance models. Note that the dynamic and equilibrium states are estimated efficiently in this method. Interestingly, every solution and its position perform as a search agent. Equilibrium candidates randomly update their positions in accordance with their best-so-far solutions. Thus, they reach the optimum solutions. The inbuilt mechanism enhances its ability to explore and exploit the solution space. Recently, an improvised version of the EO, called the adaptive equilibrium optimization (AEO) is proposed in [17]. The strength of this optimizer is its adaptive decision-making mechanism. Its performances are better than the EO, because nonperformer search agents are dispersed. Therefore, we are motivated to use the AEO for solving our problem on hand.

Initialization: Generate random position vectors C_i of the *i*-th search agents for *N* search agents for the iteration *iter* = 1.
For *iter* = 1:*max_iter*
  Compute the fitness value *fit* for the current iteration.
  Evaluate the equilibrium candidates $\vec{C}_{eq(1)}$, $\vec{C}_{eq(2)}$, $\vec{C}_{eq(3)}$, $\vec{C}_{eq(4)}$, and $\vec{C}_{eq(ave)}$.
  Build the equilibrium pool $\vec{C}_{eq,pool}$.
  Complete memory saving.
  For *i* = 1:*N*
    Randomly select the $\vec{C}_{eq}$ from the equilibrium pool $\vec{C}_{eq,pool}$.
    Build the exponential term $\vec{F}_i$.
    Build the generation rate $\vec{G}_i$.
    Build the average fitness fit_{avg}.
    Build the position search agent $\vec{C}_i(new)$.
    Update the position of search agents $\vec{C}_i$ for the next iteration.
  End (For)
End (For)
Return the best solution as $\vec{C}_{eq(1)}$, and its best fitness as $fit\left(\vec{C}_{eq(1)}\right)$.

The exhaustive search is carried out here by deploying the AEO. For ready implementation, the pseudo-code is written above.

The number of the search agents *N*, maximum number of iterations *max_iter*, search dimension *d*, and the free parameters a_1, a_2, *GP* [17] are assigned at the start. Notations are chosen from [17]. The parameters are chosen same as [17]. Our aim here is to optimize the proposed functional *f*(.) shown in (5).

4 Results and Discussions

The experiments are carried out on a core-i5 platform running under Windows 10 operating system. The algorithms are implemented using MATLAB. The same parameters are chosen for the AEO as discussed in [17]. Here, five standard test images are considered for the experiment (Img-1: Lena image; Img-2: Cameraman image; Img-3: Pepper image; Img-4: Baboon image; Img-5: Hunter image). These test images are thresholded for levels M = 2, 3, 4, and 5 using both methods. Figs. 3-7 display thresholded images for levels M =3, 4, 5 only. To conserve space, results with M = 2 are not displayed here. It is seen from the histograms of the corresponding images that they are multimodal in nature. This is the reason why they are well suited for multilevel thresholding experiment. The thresholded images are found using the following rules:

For 2-level thresholding, let us assume that $t_{1opt} = T1$; $t_{2opt} = T2$. The output segmented image $\tilde{I}$ with grey levels *0,1,2,…, L*-1 are assigned grey levels:
T, for $0 < T \leq T1$
$T1$, for $T1 < T \leq T2$ and
$T2$, $T2 < T < L$-1
This rule is extended for higher level image segmentation. The segmented outputs (results) using Tsallis entropic-value-based technique and Otsu's method are also shown here for a comparison. Note that the results obtained from our implementations of Otsu's method are presented. From Figs. 3-7, it is seen that our method yields better results than the other methods.

Tables 1 and 2 display results for five different types of images discussed above. Table 1 shows the best objective function values while their corresponding optimum threshold values are presented in Table 2. The best values are marked here with boldface numerals. From Table 1, it is seen that the suggested method yields better objective function values compared to the histogram-based methods. The reason is that the fitness functions are differently formulated. It is reiterated that our proposed one does not depend on spatial distribution. In this work (Eq. (4)), the optimal threshold values are achieved when the partition score is maximized. The count n_s directly relates to the optimal thresholds. To be more specific, maximum partition score leads to a higher objective function value. This is reflected in Table 1. In this sense, the objective functions defined in (7)-(9) are very useful for multilevel threshold selection.

Further, for validation, three different measures called – PSNR [18], SSIM [19], and FSIM [20] are considered for a quantitative validation. The PSNR of an image is the ratio of the maximum possible value (power) to the strength of distorting noise, which affects the image's representation quality. Because of the images' wide dynamic range, the PSNR is expressed in decibels (dB) (ratio between the largest and smallest possible values of a changeable quantity). PSNR is chosen as a performance indicator because it indicates signal content, which ultimately depends on the thresholded image quality. Tables 3, 4, and 5 display our results to justify the claim. PSNR values are displayed in Table 3. Table 3 depicts that the suggested technique provides a higher PSNR value compared to the other methods.

Higher the PSNR value, the better the methodology. In this work, we get higher PSNR values. For instance,

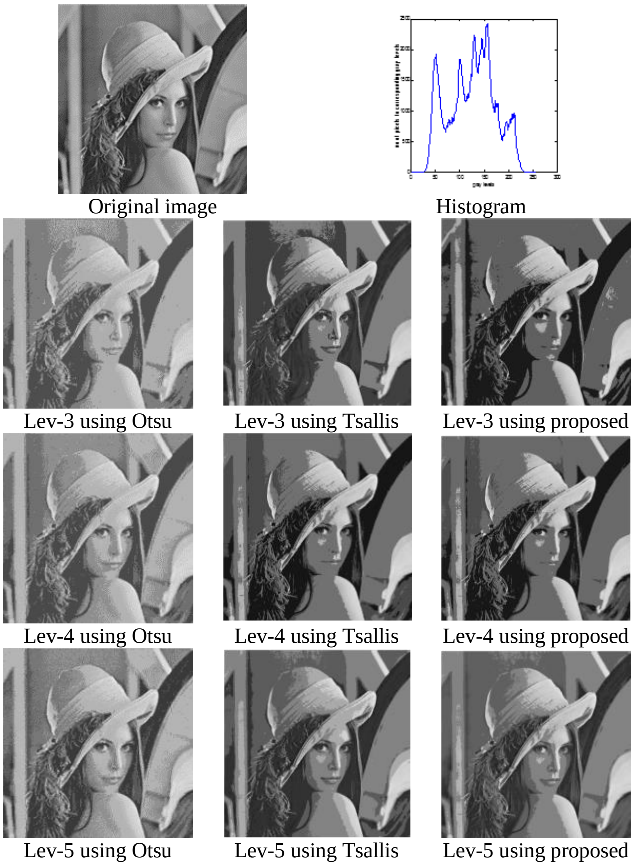

Fig. 3 Thresholded results of Img-1.

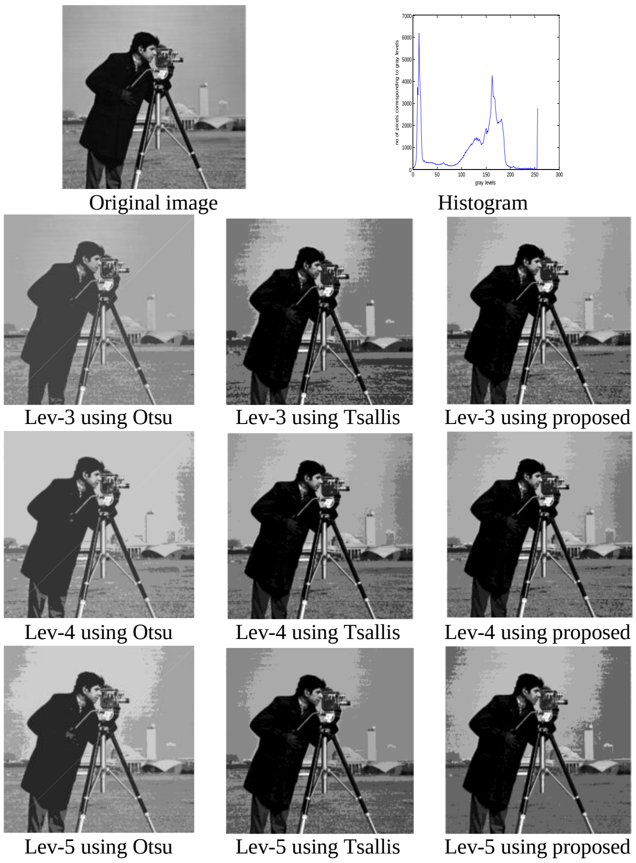

Fig. 4 Thresholded results of Img-2.

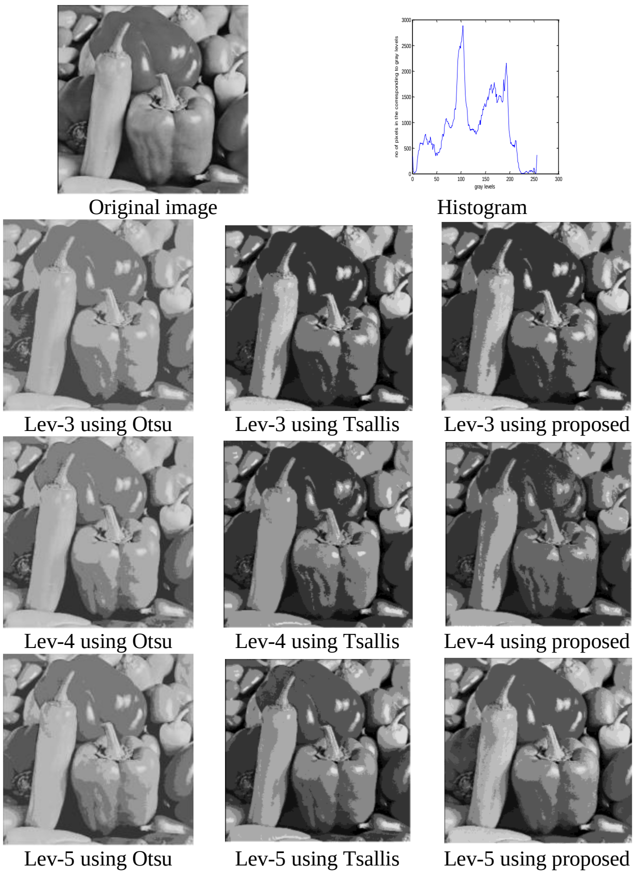

Fig. 5 Thresholded results of Img-3.

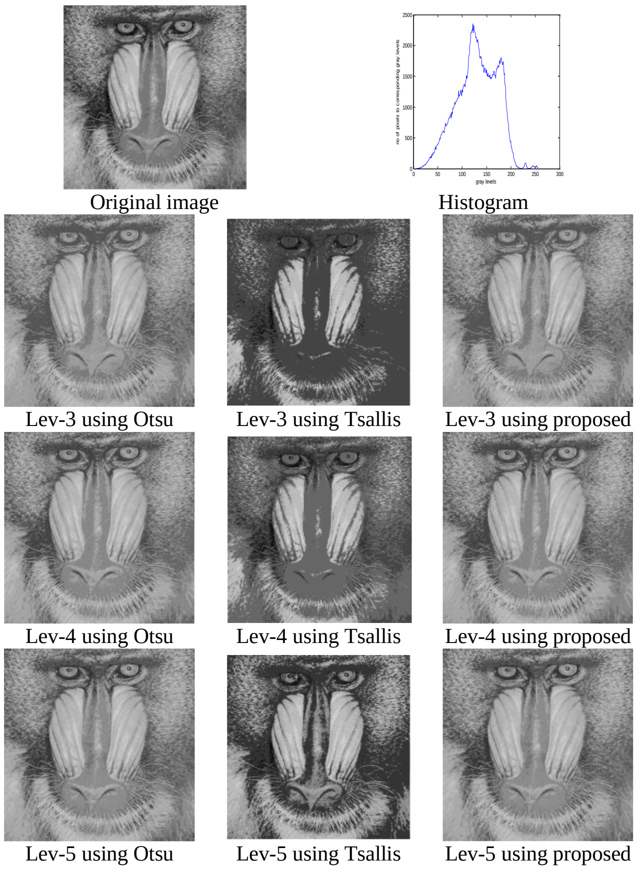

Fig. 6 Thresholded results of Img-4.

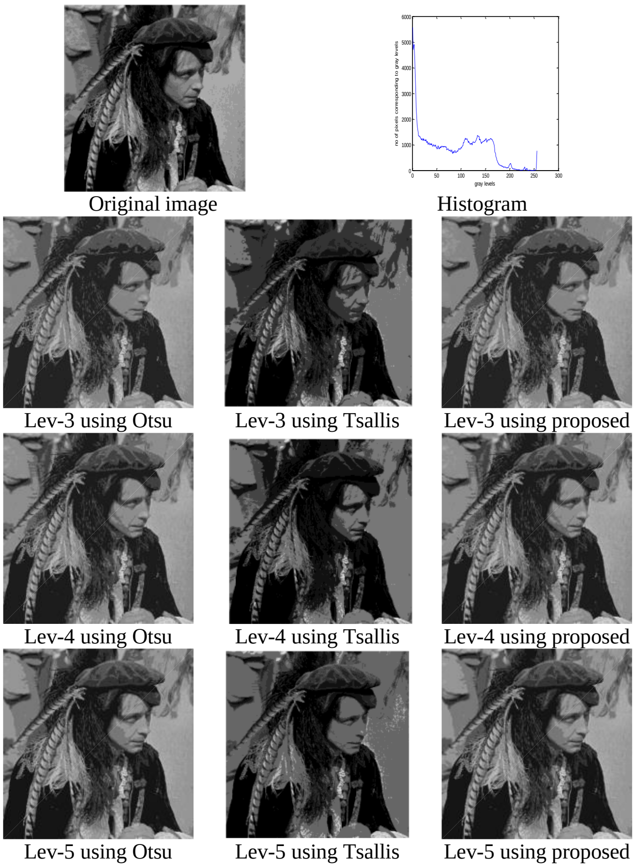

Fig. 7 Thresholded results of Img-5.

Table 1 Comparison of objective function values.

Test images	M	Objective function values		
		Proposed	Tsallis	Otsu
Img-1	2	12.3595	12.3470	11.1123
	3	15.3027	15.2206	13.6985
	4	17.9893	17.9333	16.1399
	5	20.9971	20.6099	18.5489
Img-2	2	12.5958	12.2646	11.0381
	3	15.4572	15.2507	13.7256
	4	18.5027	18.4066	16.5659
	5	21.3417	21.2111	19.0900
Img-3	2	12.6380	12.5191	11.2672
	3	16.5842	15.3998	13.8598
	4	18.4677	18.2697	16.4427
	5	21.6940	20.9999	18.8999
Img-4	2	12.2989	12.2164	10.9948
	3	15.2516	15.2114	13.6903
	4	18.0378	17.9992	16.1993
	5	20.7868	20.7200	18.6480
Img-5	2	12.5321	12.3733	11.1360
	3	15.7758	15.5533	13.9980
	4	18.4269	18.3819	16.5437
	5	21.3101	21.2565	19.1309

Table 2 Comparison of the corresponding threshold values.

Test images	M	Optimal thresholds values		
		Proposed	Tsallis	Otsu
Img-1	2	98,170	97,64	90,147
	3	71,125,180	88,142,188	78,126,174
	4	65,86,152,207	74,114,149,184	74,112,143,179
	5	35,50,138,152,207	64,95,128,163,194	58,90,120,145,180
Img-2	2	45,102	116,196	69,144
	3	36,66,145	95,139,193	66,134,168
	4	47,96,170,202	42,96,139,200	51,108,149,199
	5	27,92,190,192,250	42,84,115,150,198	39,91,136,164,205
Img-3	2	78,144	79,149	73,139
	3	58,148,194	69,100,155	69,124,172
	4	60,106,170,213	63,109,144,178	50,88,129,174
	5	1,87,127,163,256	54,89,131,164,197	52,87,121,152,182
Img-4	2	62,126	81,144	98,149
	3	60,131,147	53,112,150	85,123,158
	4	59,99,126,186	39,90,131,168	68,104,135,165
	5	57,69,123,156,198	38,79,113,148,180	53,87,115,140,168
Img-5	2	78,171	85,179	51,116
	3	71,116,174	57,104,175	35,85,133
	4	51,76,93,173	50,98,139,180	28,65,103,141
	5	43,77,94,114,202	49,93,137,179,222	21,53,87,120,150

there is an improvement of about 13.3% compared to the Tsallis method (w.r.t Lev-2 segmentation for Img-1) and about 17.2% compared to the Otsu method. Similarly, PSNR values for our method are about 30% higher than the other methods in the case of Img-5 at Lev-2 segmentation.

PSNR only quantifies the quality of a reconstructed or thresholded image in relation to ground truth. SSIM (Structural Similarity index) and FSIM (Feature Similarity index) are more powerful image structure measurement metrics. The SSIM and FSIM of a reconstructed image to ground-truth are always one, and

Table 3 Comparison of PSNR values.

Test images	M	PSNR values		
		Proposed	Tsallis	Otsu
Img-1	2	23.4362	20.6751	19.9873
	3	23.9096	22.0513	20.2347
	4	24.6523	23.4636	22.4291
	5	25.0232	24.5300	24.0455
Img-2	2	22.6829	18.7141	18.6346
	3	21.5246	20.2893	19.0142
	4	22.2643	21.8086	18.4202
	5	24.8527	22.9834	20.6539
Img-3	2	27.3341	21.1621	19.0368
	3	25.4532	23.5431	20.0117
	4	26.9922	21.5160	21.8273
	5	25.9476	22.7437	20.4693
Img-4	2	22.1818	22.1187	20.6578
	3	24.6534	23.1557	22.8167
	4	23.1703	22.0814	21.1861
	5	23.0677	22.4705	22.0529
Img-5	2	24.7929	22.6828	18.5186
	3	21.7246	21.2280	20.7661
	4	23.0956	21.6956	20.5195
	5	26.1473	20.5667	20.9837

Table 4 Comparison of SSIM values.

Test images	M	SSIM values		
		Proposed	Tsallis	Otsu
Img-1	2	0.9720	0.9528	0.7542
	3	0.9751	0.9685	0.7384
	4	0.9821	0.9789	0.8026
	5	0.9901	0.9833	0.8527
Img-2	2	0.9765	0.9417	0.7332
	3	0.9681	0.9632	0.7542
	4	0.9783	0.9756	0.7401
	5	0.9793	0.9609	0.7491
Img-3	2	0.9880	0.9555	0.8056
	3	0.9828	0.9756	0.7841
	4	0.9892	0.9671	0.8165
	5	0.9850	0.9768	0.8242
Img-4	2	0.9633	0.9605	0.7769
	3	0.9814	0.9712	0.8314
	4	0.9714	0.9711	0.8723
	5	0.9803	0.9787	0.8895
Img-5	2	0.9934	0.9715	0.6266
	3	0.9623	0.9611	0.6777
	4	0.9892	0.9648	0.7166
	5	0.9868	0.9556	0.7539

Table 5 Comparison of FSIM values.

Test images	M	FSIM values		
		Proposed	Tsallis	Otsu
Img-1	2	0.9723	0.9751	0.7974
	3	0.9733	0.9813	0.8036
	4	0.9896	0.9889	0.8537
	5	0.9921	0.9903	0.8957
Img-2	2	0.9894	0.9713	0.8409
	3	0.9871	0.9859	0.8739
	4	0.9922	0.9903	0.8723
	5	0.9977	0.9921	0.8834
Img-3	2	0.9989	0.9941	0.8260
	3	0.9927	0.9973	0.8314
	4	0.9989	0.9958	0.8737
	5	0.9985	0.9983	0.8909
Img-4	2	0.9764	0.9682	0.8742
	3	0.9798	0.9766	0.9222
	4	0.9772	0.9821	0.9506
	5	0.9820	0.9763	0.9650
Img-5	2	0.9975	0.9946	0.8306
	3	0.9963	0.9926	0.8912
	4	0.9988	0.9955	0.9190
	5	0.9990	0.9948	0.9416

a value close to one indicates that the image is of good quality. SSIM computes the visual similarity between the original image I and the thresholded image $\tilde{I}$, at a particular level. It is a comprehensive reference index, which means that image quality assessment or measurement is based on an original distortion-free image used as a reference image. It is regarded as an improvement over traditional approaches to comparison measures such as PSNR and RMSE. It is a perception-based metric that takes image deterioration into account when structural information changes. This also incorporates crucial perceptual phenomena, such as brightness masking requirements and contrast factors. It should be emphasized that structural information indicates a high degree of interaction between spatially close pixels. These dependencies communicate critical information about the image's object structure [19]. Table 4 explicitly reveals that SSIM is higher for the suggested scheme. Interestingly, the suggested method achieves results that are visually better than the entropic value-based method. FSIM is also used here to measure the similarity. The FSIM index is used to assess segmentation performance using low-level features. It makes use of two key components: phase congruency (PC) and gradient magnitude (GM), which are the first and second attributes, respectively. The PC denotes the importance of local structures [20]. Moreover, FSIM values are also higher for the suggested method, which is seen in Table 5. The detailed definitions of the performance indexes are given in the respective references.

5 Conclusions

Unlike earlier entropic value-based methods reported for multilevel threshold selection, based on Shannon's entropy information, the suggested method is based on the score among classes, which is an inventive idea on image processing. Nevertheless, an exemplar solution to the multilevel threshold selection is fostered in this paper. The justification behind the use of Tsallis objective function and Otsu function for the experiment is for a fair comparison. The non-entropic method may enrich the literature and attract more readers working in the field of AI applications to image processing. The proposed partition score ensures both qualitative and quantitative results. The proposed methodology exhibits remarkable differences as compared to the Tsallis entropic value and Otsu-based approaches (which are recently published research works). It is implicit from the results that more information is retained. Even more interesting is its simplicity. Therefore, the suggested method is quite competent and enforces its application in the area of image processing. The proposed method may also be explicitly used in high-dimensional applications. The method would be useful for thresholding of brain magnetic resonance images. This study may help researchers to explore further ideas in the field of AI applications to image thresholding.

Intellectual Property

The authors confirm that they have given due consideration to the protection of intellectual property associated with this work and that there are no impediments to publication, including the timing of publication, with respect to intellectual property.

Funding

No funding was received for this work.

CRediT Authorship Contribution Statement

G. Das: Research & investigation, Data curation, Software and simulation. **R. Panda:** Idea & conceptualization, Methodology, Supervision. **L. Samantaray:** Software and Simulation, Original Draft Preparation, Analysis. **S. Agrawal:** Revise & editing, Verification, Analysis.

Declaration of Competing Interest

The authors hereby confirm that the submitted manuscript is an original work and has not been published so far, is not under consideration for publication by any other journal and will not be submitted to any other journal until the decision will be made by this journal. All authors have approved the manuscript and agree with its submission to "Iranian Journal of Electrical and Electronic Engineering".

References

[1] M. Nixon and A. Aguado, *Feature extraction and image processing for computer vision*. Academic Press, 2019.

[2] M. Sezgin and B. Sankur, "Survey over image thresholding techniques and quantitative performance evaluation," *Journal of Electronic Imaging*, Vol. 13, No. 1, pp. 146–65. 2004.

[3] M. Portes de Albuquerque, I. A. Esquef, and A. R. Gesualdi Mello, "Image thresholding using Tsallis entropy," *Pattern Recognition Letters*, Vol. 25, No. 9, pp. 1059–1065, 2004.

[4] A. B. Hamza, "Nonextensive information-theoretic measure for image edge detection," *Journal of Electronic Imaging*, Vol. 15, No. 1, pp. 1–8, 2006.

[5] P. Y. Yin, "Multilevel minimum cross entropy threshold selection based on particle swarm optimization," *Applied Mathematics and Computation*, Vol. 184, No. 2, pp. 503–513, 2007.

[6] Z. Yudong and W. Lenan, "Optimal multi-level thresholding based on maximum Tsallis entropy via an artificial bee colony approach," *Entropy*, Vol. 13, No. 4, pp. 841–859, 2011.

[7] P. Anitha, S. Bindhiya, A. Abinaya, S. C. Satapathy, N. Dey, and V. Rajinikanth, "RGB image multi-thresholding based on Kapur's entropy—A study with heuristic algorithms," in *Second International Conference on Electrical, Computer and Communication Technologies (ICECCT)*, Coimbatore, India, pp. 1–6, 2017.

[8] A. K. M. Khairuzzaman and S. Chaudhury, "Masi entropy based multilevel thresholding for image segmentation," *Multimedia Tools and Applications*, Vol. 78, No. 23, pp. 33573–33591, 2019.

[9] A. Wunnava, M. K. Naik, R. Panda, B. Jena, and A. Abraham, "A differential evolutionary adaptive Harris hawks optimization for two dimensional practical Masi entropy-based multilevel image thresholding," *Journal of King Saud University-Computer and Information Sciences*, 2020.

[10] M. K. Naik, R. Panda, A. Wunnava, B. Jena, and A. Abraham, "A leader Harris hawk's optimization for 2-D Masi entropy-based multilevel image thresholding," *Multimedia Tools and Applications*, pp.1–41, 2021.

[11] M. Pan and F. Zhang, "Analysis of the α-Renyi entropy and its application for medical image registration," *Biomedical Engineering, Applications, Basis and Communications*, Vol. 29, No. 03, p. 1750020, 2017.

[12] A. D. Brink, "Minimum spatial entropy threshold selection," *IEE Proceedings-Vision, Image and Signal Processing*, Vol. 142, No. 3, pp.128–132, 1995.

[13] P. D. Sathya, R. Kalyani, and V. P. Sakthivel, "Color image segmentation using Kapur, Otsu and Minimum cross entropy functions based on exchange market algorithm," *Expert Systems with Applications*, Vol. 172, p. 114636, 2021.

[14] B. Lei and J. Fan, "Multilevel minimum cross entropy thresholding: A comparative study," *Applied Soft Computing*, Vol. 96, p. 106588, 2020.

[15] T. Pun, "Entropic thresholding, a new approach," *Computer Graphics and Image Processing*, Vol. 16, No. 3, pp. 210–239, 1981.

[16] A. Faramarzi, M. Heidarinejad, B. Stephens, and S. Mirjalili, "Equilibrium optimizer: A novel optimization algorithm," *Knowledge-Based Systems*, Vol. 191, p. 105190, 2020.

[17] A. Wunnava, M. K. Naik, R. Panda, B. Jena, and A. Abraham, "A novel interdependence based multilevel thresholding technique using adaptive equilibrium optimizer," *Engineering Applications of Artificial Intelligence*, Vol. 94, p.103836, 2020.

[18] L. Samantaray, S. Hembram and R. Panda, "A new Harris hawks-cuckoo search optimizer for multilevel thresholding of thermogram images," *Revue d'inteliigence Artificiele*, Vol. 34, No. 5, pp. 541–551, 2020.

[19] Z. Wang, A. C. Bovik, H. R. Sheikh, E. P. Simoncelli, "Image quality assessment: from error visibility to structural similarity," *IEEE Transactions on Image Processing*, Vol. 13, No. 4, pp. 600–612, 2004.

[20] L. Zhang, L. Zhang, X. Mou, D. Zhang, "FSIM: A feature similarity index for image quality assessment," *IEEE Transactions on Image Processing*, Vol. 20, No. 8, pp. 2378–2386, 2011.

G. Das received his B.Tech. degree from NIT Bhopal in 1998 and M.Tech. degree from BPUT, Rourkela in 2010. Currently, he is pursuing his Ph.D. in Engineering in VSS University of Technology, Burla. His research interests include signal/image processing, soft computing, and AI.

R. Panda was born in 1963. He received B.Sc. and M.Sc. degrees from UCE Burla in 1985 and 1988, respectively. He obtained Ph.D. degree from IIT, KGP in 1998. He is currently a Professor in the Department of Electronics and Telecommunication Engineering, VSS University of Technology, Burla. He was the former HOD ECE Dept., HOD CSE Dept., DEAN, Academic Affairs, DEAN, SRIC, and DEAN Continuing Education Programme. He has guided 37 M.Tech. Theses and 8 Ph.D. Theses. He has over 170 papers in International/National Journals and conferences. Dr. Panda has more than 1900 academic citations with h-index of 24 and i10-index of 43 as per Google scholar. He is the co-author of a book titled "AI Techniques for Biomedical Engineering Applications" and 8 Book Chapters. He is a member of IEEE and a Fellow of IETE (India). He is the reviewer of many reputed international journals like IEEE Transactions and Elsevier Journals. He received "Highly Cited Research Award" in Dec. 2016 from Swarm and Evolutionary Computation Journal, Elsevier. He received "Certificate of Appreciation Award" for quality research Journal Publications for the year 2020 from VSS University of Technology, Burla. His one article is found in the top ten popular articles of IEEE Reviews in Biomedical Engineering. His area of research interests includes digital signal/image processing, bioinformatics, biomedical engineering, VLSI signal processing, soft computing, machine intelligence, and AI.

L. Samantaray received her B.E. degree from BPUT, Rourkela in 1996, M.Tech. degree from UCE Burla in 2001. She obtained her Ph.D. degree from Sambalpur University in 2010. She is currently a Professor in the Department of Electronics and Communication Engineering, Ajaya Binaya Institute of Technology, Cuttack. She has guided 2 M.Tech. Theses. She has over 30 papers in International/National Journals and Conferences. Dr. Samantaray is the co-author of 3 Book Chapters. She is a member of IEEE. Her area of research interests includes digital signal/image processing, biomedical engineering, soft computing, machine intelligence, and AI.

S. Agrawal was born in 1972. He received B.E. and M.Tech. Degrees from UCE Burla in 1995 and 2003, respectively. He obtained Ph.D. degree from Sambalpur University in 2015. He is currently an Associate Professor in the Department of Electronics and Telecommunication Engineering, VSS University of Technology, Burla. He has guided 18 M.Tech. Theses and 3 Ph.D. Theses. He has over 40 papers in International Journals and Conferences. Dr. Agrawal has more than 800 academic citations with h-index of 14 and i10-index of 14 as per Google scholar. He is the co-author of a book titled "AI Techniques for Biomedical Engineering Applications" and 8 Book Chapters. He is a member of IEEE. His area of research interests includes digital signal/image processing, bioinformatics, biomedical engineering, soft computing, machine intelligence, and AI.